Applied Energy 184 (2016) 40–54

Contents lists available at ScienceDirect

Applied Energy

journal homepage: www.elsevier.com/locate/apenergy

A city scale degree-day method to assess building space heating energy demands in Strasbourg Eurometropolis (France)

M. Kohler [a,b,*], N. Blond [a], A. Clappier [a]

[a] Laboratoire Image Ville Environnement, CNRS UMR 7230, Université de Strasbourg, 3 rue de l'Argonne, 67000 Strasbourg, France
[b] Leibniz Institute of Ecological Urban and Regional Development, Weberplatz 1, 01217 Dresden, Germany

HIGHLIGHTS

- Energy profiles are numerically modeled at city scale.
- They integrate the urban heat island complexity and building internal heat gains.
- Based on degree-days a fast energy management tool for urban planner is then framed.
- Reliable estimates of urban-scale building energy loads are obtained.
- Degree-day daily temperature definition causes the largest results' discrepancies.

ARTICLE INFO

Article history:
Received 20 June 2016
Received in revised form 18 September 2016
Accepted 26 September 2016

Keywords:
Building space heating energy
Urban heat island
Degree-day method

ABSTRACT

Efficient strategies are required to reduce space heating energy demands in buildings at city scale. Models taking into account the dynamic of the Urban Heat Island (UHI) phenomenon may be useful tools to help urban planners in this task. In this paper, we propose a new methodology to assess the energy demands for space heating in buildings at city scale: a degree-day method is applied, coupled with the use of a dynamic urban meteorological model that computes a building energy budget. First, it is shown that the total building space heating energy demand at city scale, as simulated by the meteorological model, is quasi- linearly dependent on the daily mean city scale air temperature. The developed city-scale degree-day method applied to assess the space heating energy demands in Strasbourg Eurometropolis (France) is shown to be consistent with the estimates issued by local official energy sources. A sensitivity analysis highlights the fact that while the heating energy demands are dependent on the building insulation performance and thermostat heating temperatures, scenarios in which building energy properties are changed do not significantly affect the UHI.

1. Introduction

Predictions of energy demands for buildings are extremely useful to energy suppliers' wishing to optimize of the energy supplies and introduce renewable energy to the electricity mix [1]. Now that the potential of buildings to contribute towards reductions in the carbon dioxide (CO_2) emissions is well recognized [2–4], urban planners require predictions of the building energy demands to assess the impact of energy conservation measures. Such measures can target building properties, helping to achieve direct cooling/heating energy savings by the appropriate use of building materials and compact designs [5], as well as parcel designs, thereby contributing towards voluntary man-managed microclimate variations within cities and indirect cooling/heating energy savings [6].

Urban areas usually experience higher external air temperatures and reduced natural ventilation compared to rural countryside. This is due to a combination of factors: waste heat released to the atmosphere through human activity; reduced sky view factors due to high building density; higher heat capacity of built-up materials; and a lack of evaporative cooling areas. This concentration of factors produces the phenomenon known as the Urban Heat Island (UHI) [7]. Typical urban-rural temperature anomalies range from +2 to +7 K [8]. Due to UHI, building space cooling (heating) energy demands are usually higher (lower) in very dense city districts than in the green suburbs [8]. With the warming of the global climate, urban planners are increasingly looking to UHI mitigation measures in order to reduce energy demands for building cooling.

* Corresponding author at: Laboratoire Image Ville Environnement, CNRS UMR 7230, Université de Strasbourg, 3 rue de l'Argonne, 67000 Strasbourg, France.
E-mail address: 1kohlerm@gmail.com (M. Kohler).

http://dx.doi.org/10.1016/j.apenergy.2016.09.075
0306-2619/

However, one case study in London (Oceanic climate) and a second in Athens (Mediterranean climate) have suggested mixed results of UHI mitigation strategies on annual energy demands for buildings [9,10]. In these two studies, UHIs are shown to basically contribute to annual energy savings in buildings by greatly reducing energy demands for space heating (around −30%) in comparison to a much smaller increase in energy required for indoor cooling (+13%). Thus it is vital to assess more precisely the effects of UHI mitigation measures on energy requirements for both building space heating and cooling [11,12]. The present study will focus only on the energy demands for space heating.

Many modeling techniques can be used to predict the annual energy demands at city scale for buildings space heating. These differ in regards to their trade-off between the degree of complexity, level of details in their input data, and processing time [13]. A subsequent review of current model can be found in Swan and Ugursal [14], Kavgic et al. [15], and Wang et al. [16].

At the scale of the buildings, engineering building energy models such as the US Department of Energy's EnergyPlus software (http://apps1.eer.energy.gov/buildings/energyplus/) or TRNSYS software (www.trnsys.com) have been extensively used in bottom-up building energy models to inform demand profiles for space heating energy (expressed in W h/capita or m^2) of specific building types [17,18]. Based on a classification of the urban housing stock into building types [19–21], the basic idea of these models is to multiply the heating energy demand profiles of each building types by their respective ratio in the city housing stock to get the total space heating energy demands for buildings at city scale. Although engineering building energy models take pains to consider quasi-real building geometries, separate thermally homogenous zones inside the building, complex layered wall and glazing systems, shading systems, as well as solar and occupant passive heat gains, they have been shown to overestimate space heating energy demands by considering buildings as stand-alone entities [22]. According to Pisello et al. [23], neglecting the mutual thermal dynamics interactions between buildings (one factor behind UHI) can lead to substantial overestimates of space heating energy demands by up to +22%. Therefore, some scholars have proposed forcing engineering building energy models with empirical weather observations measured along city transects [9,10,12] or urban temperature data reconstructed from rural observations [24].

At the city or regional scale, degree-day methods are the simplest way to take inter-annual temperature variability into account when estimating or predicting annual space heating energy consumptions without performing complex calculations [18,25–28]. In static conditions, the heat losses from one particular building are observed to be directly proportional to the differences between the building outdoor temperatures and a reference temperature (the base temperature), below which buildings need space heating energy to maintain conditions of thermal comfort [29]. This relation is used to assess the annual heating energy demands, which are then calculated using regional building energy loss rates and the sum over a fixed time period of the differences between the mean daily air temperatures and a base temperature. This sum is called the Heating Degree Day (HDD). It captures the variations of such an indoor and outdoor temperature gradient over a fixed time period.

There are several ways to determine the HDD: from long-term hourly temperature records, mean daily temperatures, daily maximum and minimum temperatures, to mean monthly temperatures and their standard deviations [30–32] or following Giannakopoulos et al. [33], using global climate numerical simulations. The finer is the grain of the temperature dataset, the more accurate the HDD. However, all these approaches do not take into account the impact of UHI. Studies using synoptic meteorological records monitored at the urban outskirts or which employ coarse meteorological simulation grid resolutions neglect the effect of the urban environment on local temperatures.

Despite these advances at various scales, we will need fast and robust models able to assess annual space heating energy demands for buildings at city scale while taking into account the dynamic of the UHI.

Since the 2000s, sophisticated three-dimensional urban canopy parameterizations (UCPs) and energy models have been introduced in mesoscale atmospheric models [34–36]. The framed system of urban climate models now makes a trade-off between a relatively high level of accuracy of the description of the housing stock and urban surface heterogeneity with relatively fast processing times. In grid cells of 1–5 km, these UCPs calculate the average three-dimensional effects of simplified cubic building geometries on the atmospheric energetics and dynamics by taking account of the mutual energy interactions between buildings (solar radiation and wind sheltering effects, longwave thermal radiation multi-reflections), as well as the total building space heating and cooling energy demands. The space heating energy demands are calculated from the indoor energy budget by considering diurnal variations in internal energy gains (due to the solar heat and standard building operation) and the energy losses (due to the building natural ventilation and wall energy transmissions) along with standard expectations of indoor thermal comfort.

Until now, only a few studies have already used such urban climate modeling systems to predict energy demands for building space heating. Salamanca et al. [37] have applied such a modeling system to assess the outcome of energy saving strategies over several days in Madrid. Masson et al. [38] have assessed the influence of current strategies on urban densification and greening on the energy demand for building space heating and cooling of the Toulouse housing stock in the year 2100. Martilli [39] has investigated the effect of the urban structure (building height, density, green covers) on the space heating and cooling energy demands by considering successively a simplified and a theoretical city geometry. These studies have shown that while such urban climate modeling systems perform well in estimating the space heating and cooling energy demands, in particular taking account of intermittent space heating, the complex calculations involved require considerable processing power and time. To resolve this problem, especially when long-term simulations are needed, the simulation runs are usually limited to relevant short periods [40,41], offline UCP runs [42], or the models are simplified [38,43–45].

The present study aims to demonstrate the capacities of a new approach that combines such an urban climate modeling systems with a degree-day method in estimating annual energy demand in buildings for space heating of a given city or urban territory. The method is notably illustrated by a case study of Strasbourg Eurometropolis (France), for which official energy data is available for validation. The novelty of the proposed study is in applying the classical energy signature method used in the degree-day methods at the scale of a city or an urban territory using a physically based numerical urban meteorological model that integrate the buildings' mutual energetic interactions and their effects on the atmospheric energetics and dynamics (UHI effects). Of course, first we have to ensure that the quasi-linearity of the space heating energy demands with the outdoor air temperatures is still valid according to our methodology. This numerical approach enables in particular the generation of a large dataset on urban temperatures and space heating energy demands all over the world suitable for energy signature methods and improved determination of HDD values (city scale base temperature and building heat losses). Unlike other numerical studies that require a large data input and considerable computing skills, our city-scale degree-day model once established provide a suitable tool for urban planners to quickly assess city-scale building energy demand for space heating.

The paper is divided into five sections. Section 2 provides details of the city-scale degree-day method. Section 3 presents the Strasbourg Eurometropolis study case on which the method is applied. In Section 4 we discuss the estimates of space heating energy demands estimations and the sensitivity to building thermal performance properties. Finally, some conclusions are provided in Section 5.

2. Methodology

The methodology is derived from the classical degree-day method usually applied at building scale, but also at the scale of the regional housing stock (*e.g.* [27,28]. This classical method assumes that the energy demands for building space heating, Q_J over a period J are directly proportional to the building heat losses that may vary with the change in the current indoor-outdoor air temperature gradient (*i.e.* natural ventilation and air infiltration, wall heat conduction, thermal radiation losses). The constant of proportionality is P (in MW h/°C), which is the building's overall rate of heat loss.

Hence, the total space heating energy demand over the period of interest, Q_J, is calculated as:

$$Q_J = P * HDD_J \tag{1}$$

with, $\mathrm{HDD_J}$ the Heating Degree-Days over the period J computed as:

$$HDD_J = \sum_{t=0}^{t=J} min[(T(t) - T_0) * \Delta t; 0] \tag{2}$$

Depending on the study approach, the daily mean air temperatures $T(t)$ can either be calculated as the average of the hourly temperatures measured over a day, the daily minimum or maximum temperatures, or the mean monthly temperature and standard deviation [46], or the average of the daily maximum and minimum air temperatures [18]. While the total heat losses from the buildings are related to the actual indoor air temperature, it does not follow that all these heat losses are compensated by the heating system. Rather some are balanced by additional heat gains inside buildings from solar heating, as well as human activity or through artificial lighting, and other technical equipment. The base temperature, T_0, is specified as the outdoor air temperature at which buildings are in thermal equilibrium with their surroundings.

At regional or city scales, classic performance line or energy signature methods inform the city-scale degree-day values, namely the city-scale base temperature $\mathrm{T_{0,city}}$ and the overall building heat loss rate P_{city}. These methods consider the best fit of plots of (usually monthly) space heating energy consumption records provided by energy companies for each fuel, respectively, monthly heating degree-days calculated from several predefined base temperatures and monthly daily mean air temperature records [27,47,48]. Therefore, the accuracy of the degree-day values (*i.e.* T_0 and P) may vary with the extent of the historical regional energy and climate records as well as their resolutions. However, classical energy signature methods are being challenged by climate change. On the one hand, the shift from gas- or oil-fired furnaces and boiler heating systems towards electric heating systems more adapted to meet the demand for cooling energy undermines the assumptions on which these methods are based (*i.e.* gas and fuel energy meets the demand for space heating energy, while electrical energy meets the demand for space cooling energy). On the other hand, the base temperatures and the building heat loss rates may vary in line with more stringent building efficiency standards and new household thermal comfort expectations in buildings [49]. This will require more frequent calculation of degree-day values.

The novelty of the proposed study is in applying the classical energy signature method at the scale of a city or an urban territory using a physically based numerical urban meteorological model. Following sections details the computation of the method.

2.1. Use of an urban climate model calculating a building energy budget

Our method is based on the non-hydrostatic regional Weather and Research Forecasting model (WRF/ARW; [50]) and its Building Effect Parameterization (BEP; [51]) and Building Energy Model (BEM; [36]). BEP computes the turbulent momentum, energy, and moisture exchange between the surface and the atmosphere induced by the three-dimensional building obstacles. In contrast to real urban geometry, the obstacles are uniformly distributed in space and their complex building geometries are simplified into volume equivalent cubes. Because BEP considers reduced turbulent exchanges in streets, the mutual radiative interactions between buildings and streets (shading of the surface, longwave radiation multi-reflection), as well as the differential surface energy budgets of building facets (*i.e.* the differential heating and cooling of building facets induced by building facets' energy losses and gains from net solar and longwave radiations, latent and sensible heat fluxes, as well as by the amount of energy stored and transferred in the building materials), BEP helps to accurately compute hourly vertical air temperature profiles within cities.

As a function of the synoptic meteorological conditions and the local influence of city given by BEP, the Building Energy Model (BEM) computes the energy budget for each floor of an occupied standard building and the way the resulting energy is exchanged with the building's surroundings. The model accounts for the solar heating through the windows, heat conduction through complex layered wall systems, unintentional natural ventilation, and waste heat generated by the building occupants and equipment. According to this energy budget, BEM calculates the hourly building space heating energy demands necessary to meet a user-defined expectation of thermal comfort.

2.2. Computation of the city-scale daily mean air temperatures and space heating energy demands

Given the hourly energy demands for building heating and hourly air temperatures (taken at 2 m from ground) simulated by the non-hydrostatic version of the WRF/urban climate modeling system, it is possible to compute (following [36] the daily mean air temperatures and space heating energy demands of the buildings relevant for an urban region of interest. The city scale daily mean air temperatures are the 24-h average of the simulated hourly 2 m air temperatures of all urban grid cells in the urban region. Likewise, the city scale daily space heating energy demands are the sum over 24 h of the simulated hourly space heating energy demands of all urban grid cells in the urban region.

2.3. Deduction of the city-scale degree day model

Finally, the plot of the city scale daily space heating energy demands against the city scale daily mean air temperatures generates the energy signature profile of the urban region of interest. The slope of the best linear fit of the energy signature profile provides the global building heat loss rate $\mathrm{P_{city}}$ of the urban region, while the intercept term is nothing else than the global base temperature $\mathrm{T_{0,city}}$ of the housing stock of the urban region. Hence and as soon as P_{city} and $T_{0,city}$ are estimated, the building heating energy demands can be quickly computed using Eq. (1). The process of the city-scale degree-day method is sketched in Fig. 1.

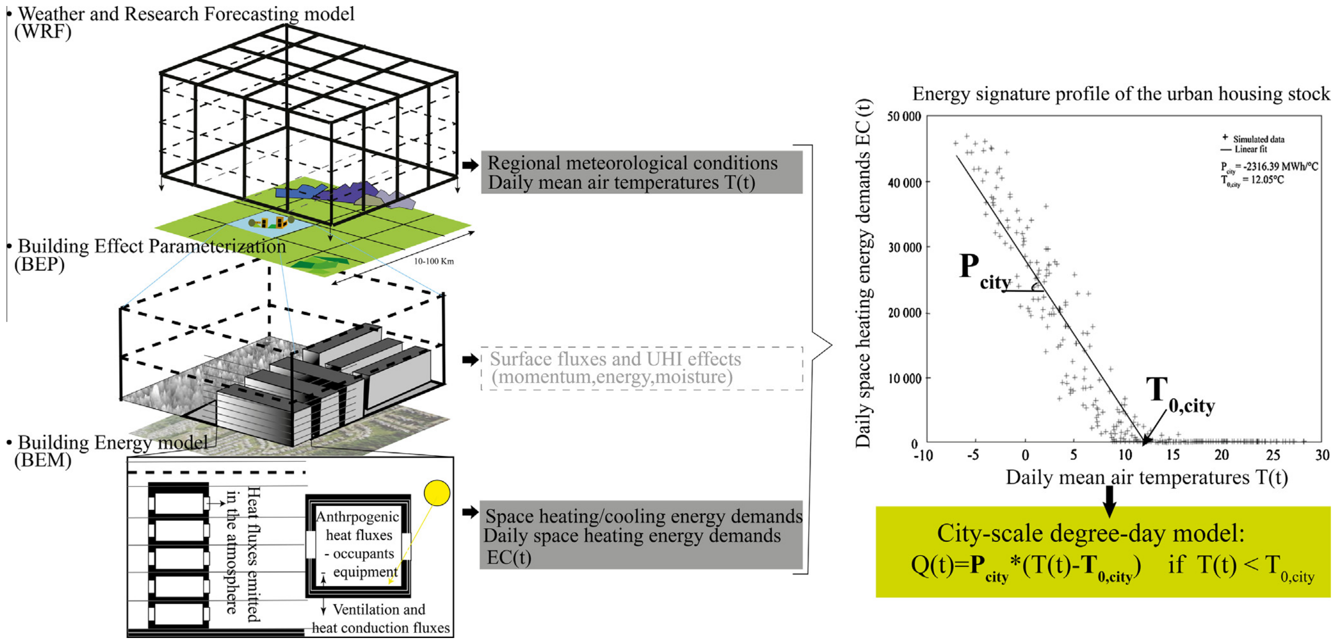

Fig. 1. The city-scale degree-day method.

Because the WRF/urban climate modeling system resolves the entire building energy budget, the deduced building heat loss rate and base temperature directly account for the energy storage within the building fabric, the internal passive heat gains, and hence, intermittent space heating in buildings.

3. Application of the methodology to the Strasbourg Eurometropolis

3.1. Area of interest: the Strasbourg Eurometropolis

The Strasbourg Eurometropolis (48°35′05″N, 7°45′02″E, and elevation: 132–151 m, Fig. 2) is a French urban community administrative body that is composed by the main Strasbourg urban pole and its 27 smallest satellite municipalities. The total size of the Strasbourg Eurometropolis territory is 316 km^2 large. As a main regional urban metropolis, the Strasbourg Eurometropolis has 483,000 inhabitants, *i.e.* 45% of the active population of the Bas-Rhin district. Most jobs are provided by high-skilled tertiary and industrial sectors (http://www.strasbourg.eu/fonctionnement-ville-cus/communaute-urbaine-strasbourg/presentation-cus). The synoptic climate is oceanic (Köppen type Cfb) with well-defined seasons: moderately cold and foggy winters (30 days of snow and 56 foggy days per year) with continental climate influence in summers. Winds are low to moderate, and due to the channeling effect of the Rhine valley often flow north to south. Consequently, the study area is characterized by a high energy demands for space heating [52].

For the purpose of this study we collected a regional inventory of building energy consumptions for space heating from the regional air quality agency (ASPA, Association pour la Surveillance, la qualité, et la Protection de l'air en Alsace; source: ASPA-1212203-TD). This inventory was constructed for the year 2010 following a bottom-up approach. Classification of the regional housing stock was first undertaken using the dwelling database of the national statistics institute INSEE, in which figures energy performance variables (*i.e.* building age, housing types, floor area and inhabitant density, as well as the nature of the heating system and fuels) for dwellings. This was used to produce energy performance dwelling profiles at district scale. Subsequently, each energy performance dwelling profile was multiplied by its respective space heating energy demand profile from the national energy observatory CEREN and weight in the district to calculate the energy consumptions for space heating for each city district of the study area [52]. A climatic factor was also introduced to account for the variation of the regional climate due to local topography (the Vosges Mountains and the flat area of the Rhine valley) and its influence on the space heating energy consumptions. This climatic factor was calculated (in the same way as the heating degree-days HDD), as the sum over a predefined heating period (by convention from 1 October to 31 May) of the differences between a daily mean temperatures and a predefined base temperature of 17 °C. The daily mean temperatures were calculated from the maximum and minimum daily air temperatures outputted from the MM5 mesoscale atmospheric model of Grell et al. [53], considering an atmospheric grid cell resolution equal to 3 km and no three-dimensional UCPs. The total space heating energy consumption for the study area was estimated at 4242987.5 MW h.

As a recent and official source of data on space heating energy consumptions, the ASPA inventory will serve as a basis for discussions on the accuracy of our methodology.

3.2. Use of the WRF/urban climate modeling system and settings

The WRF/urban climate modeling system was applied to the Strasbourg Eurometropolis. Simulations were performed for the year 2010, for which a regional inventory of the building energy consumptions was available. Globally, 2010 was one of the warmest years according to data stretching back 130 years; at the same time it was also one of the coldest years of the two last decades, according to Météo-France, the French meteorological institute.

3.2.1. Design of the base case

To take account of atmospheric conditions, the Dudhia [54] model, the Rapid Radiative Transfer model as well as the Thompson et al. [55] microphysics scheme were chosen to account for scattered radiation due to the presence of clouds and other

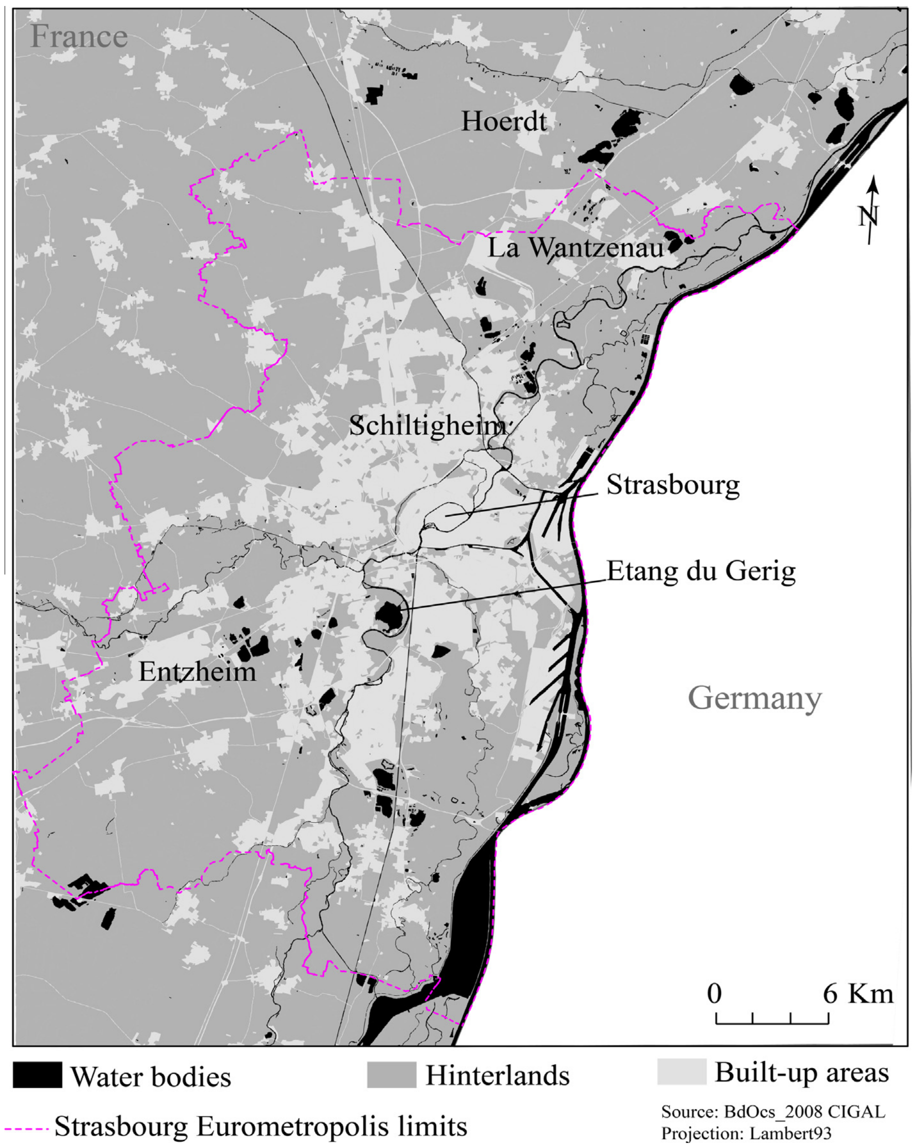

Fig. 2. Map of the Strasbourg Eurotropolis territory.

hydrometeor while the Bougeault and Lacarrère [56] Planetary Boundary Layer scheme permitted better consideration of the obstacle effects of buildings on turbulent airflows.

The gridded horizontal domain was composed of four two-way nested embedded domains with grid resolutions ranging from 45 km, 9 km, 3 km to 1 km (Fig. 3a). In a vertical direction, 27 eta-levels were defined with the pressure at the top level set at 5000 Pa. Ten of them are directly included in the first 1.5 km, and allow the urban canopy layer to be accurately described. The initial and boundary conditions of the coarsest domain were provided by the final meteorological global data reanalysis (FNL-reanalysis) of the operational National Center for Environment and Prediction (NCEP) every 6 h according to a grid resolution of 30 arc seconds. As domains are embedded, the lower resolved domains give boundary conditions to the higher resolved domains during simulations. Two-way nesting is only used for the final two domains.

The static physical conditions of the atmospheric grid cells (*e.g.* surface albedo, surface emissivity), which are also used to compute the surface energy, momentum, and moisture fluxes and longwave radiations losses from the surface, were drawn from the regional Alsatian spatial information cooperation CIGAL land use land cover database (Fig. 3b). This database compiles multisource spatial information from the SPOT 5 satellite images, the orthophotographs of the national geographical services IGN, and city cadastral maps, which accuracy is of meters.

Surface fluxes were computed using the Noah land surface model (Noah-LSM; [57] for the non-built up areas and the BEP + BEM module for the built-up areas. The BEP + BEM module allows the definition of three urban types: the high intensity residential areas (HIR), characterized by high population density and construction surface, low intensity residential areas (LIR), where buildings and built-up areas are interspersed with vegetation (representing 30–80% of the atmospheric grid area, and the commercial and industrial estates (COI). High-resolution national geographic databases have been compiled (IGN *BDtopo*®) using Geographic Information System (GIS) geoprocessing to specify the building geometry of the three urban types suitable for European cities. Relevant parameters are given in Table 1.

Two multilayered wall and roof systems have been designed for in the COI, on the one hand, and for HIR and LIR, on the other hand. For HIR and LIR, the roofs thickness is 0.16 m

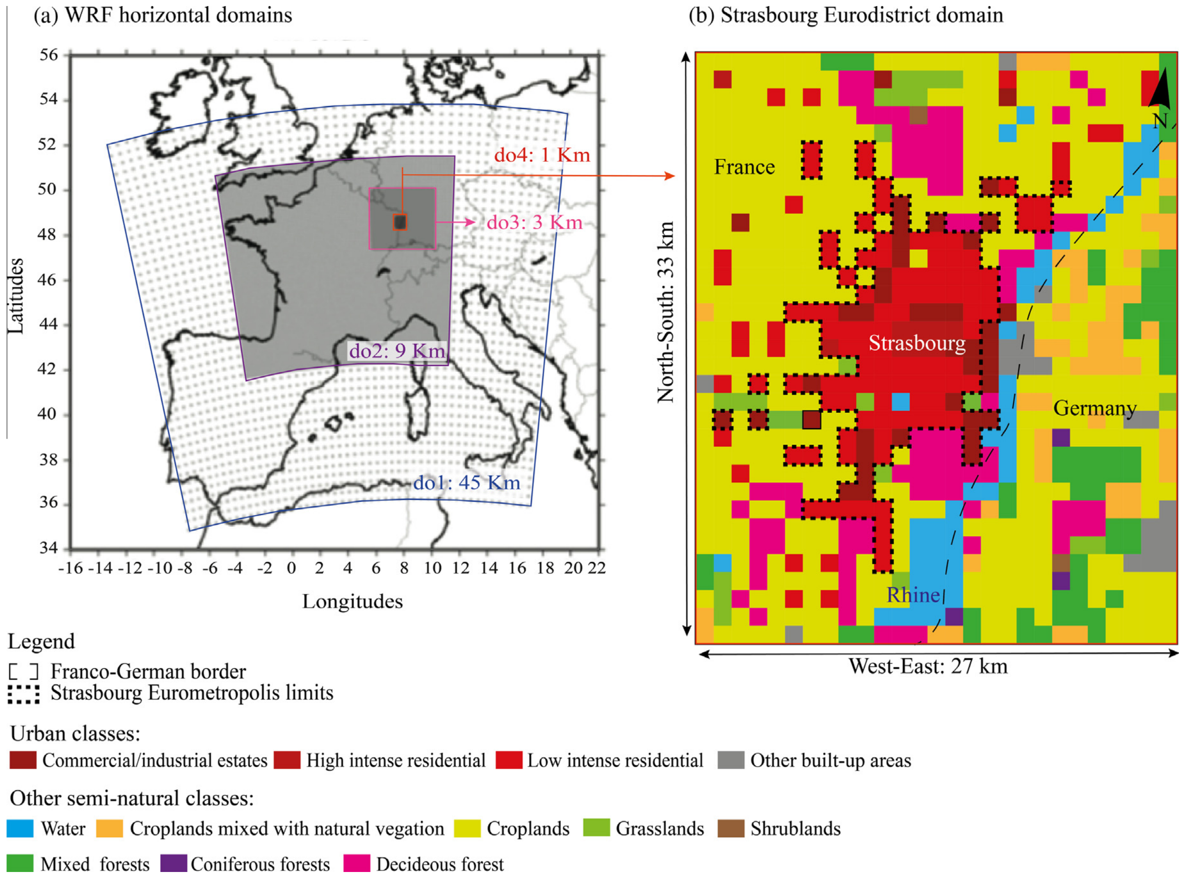

Fig. 3. (a) The four embedded atmospheric horizontal domains. (b) The Strasbourg Eurodistrict land cover as determined by the WRF/urban climate modeling system.

Table 1
Urban morphological parameters for every urban types (HIR: high intensity residential city districts; LIR: low intensity residential city districts; and COI: commercial and industrial city estates).

Parameters	HIR	LIR	COI
Floor height (m)	3	3	3
Building 5 m tall (%)	25.0	42.0	30.0
Building 10 m tall (%)	54.0	51.1	49.0
Building 15 m tall (%)	11.0	5.0	13.0
Building 20 m tall (%)	5.0	1.3	4.0
Building 25 m tall (%)	4.0	0.4	2.0
Building 30 m tall (%)	1.0	0.1	1.0
Building 40 m tall (%)	0.0	0.1	1.0
North/South street-canyon direction (°)	315	45	0
West/East street-canyon direction (°)	45	315	90
Street width in the North/South direction (m)	5	20	25
Street width in the West/East direction (m)	7	18	50
Building width in the North/South direction (m)	25	10	30
Building width in the West/East direction (m)	30	20	70

Table 2
Radiative, aerodynamic and thermal (heat diffusivity and capacities) properties of building materials used in BEP + BEM for every urban type (HIR: high intensity residential city districts; LIR: low intensity residential city districts; and COI: commercial and industrial city estates). Values from Krpo [75] and http://www.maison.com/architecture/maison-basse-consommation/bibliotheque-materiaux-construction-4818/.

Materials	Heat diffusivity ($m^2\,s^{-1}$)	Specific heat capacity ($J\,m^{-3}\,K^{-1}$)
OSB	0.13×10^{-6}	0.98×10^{6}
Air	22.90×10^{-6}	1.21×10^{6}
Vapor check membrane	7692.30×10^{-6}	0.29×10^{6}
Glasswool (18 kg/m^3)	2.37×10^{-6}	0.01×10^{6}
AGEPAN	58.33×10^{-6}	1.29×10^{6}
Brown tile	0.59×10^{-6}	0.65×10^{6}
Gypsum (BA13)	0.30×10^{-6}	0.83×10^{6}
Standard performed bricks	0.59×10^{-6}	0.65×10^{6}
Roughcast in cement	0.48×10^{-6}	1.64×10^{6}
Concrete	1636.90×10^{-6}	2.16×10^{6}

(U-value 0.21 $W\,m^{-2}\,K^{-1}$), the wall thickness 0.38 m (U-value 0.49 $W\,m^{-2}\,K^{-1}$; calculation follow [58], the floor 0.6 m (U-value 0.19 $W\,m^{-2}\,K^{-1}$), and the underground 0.96 m (U-value 0.23 $W\,m^{-2}\,K^{-1}$). The roofs are constructed of brown tile, Oriented Strand Board (OSB) and Agepan® wood fiber board, and are protected by a 9 cm glasswool layer and a waterproof membrane. Walls are made of 20 cm perforated standard bricks that are insulated by two cavity layers of air and a glasswool layer. Finally, a roughcast in cement covers the building exterior. The floors and ceilings are constructed of concrete slabs, insulated with glasswool. For the COI, walls (U-value 0.66 $W\,m^{-2}\,K^{-1}$) are made of successive layers of gypsum, air, glass wool insulation, and concrete materials. Roofs are made of concrete material protected by one air cavity layer and glasswool insulation material (U-value 0.31 $W\,m^{-2}\,K^{-1}$). The thermal properties of the materials are given in Table 2. Albedo, emissivity and roughness length for roofs are respectively set to 0.1, 0.9, and 0.01 m; for streets to 0.05, 0.95, 0.01 m; and for walls, albedo is 0.2 and emissivity is 0.9. The windows are composed of two panes of glass of width 6 mm. The heat conductivity coefficient for the windows is 5.62 $W\,m^{-1}\,K^{-1}$.

Finally, the thermostat temperature setting for heating was fixed at 19.85 °C, a comfortable temperature in dwellings usually prescribed by the French public authorities, yet which may be considered low by some people [59]. Because there is little energy demand for indoor space cooling across the study area, we discarded the air-conditioning system from the WRF/urban climate modeling system. Other parameters were defined: a ventilation rate of 0.75, the ratio of windows to walls at 0.20 for COI buildings following Salamanca et al. [60], and 0.15 for HIR and LIR. The energy efficiency of the heating system was set to 0.9 like Martilli [39] as this coefficient value also represents the average energy efficiency of all the heating systems (*i.e.* gas and fuel fired boilers, electrical resistance heater, heat pump, and so on) installed in the Strasbourg Eurometropolis' dwellings. The floor population densities were initially defined by calculating the total population over the study zone in 2010 by using the 1999 INSEE population census and linear growth rates from INSEE [61]. The total population was then calculated in proportion to the floor area across the Eurodistrict simulation domain and compiled for each urban type. This results in a floor population density equal to 6.86 individuals/100 m^2 for HIR, 1.02 individuals/100 m^2, for LIR, and 0.31 individuals/100 m^2 for COI. The metabolic heat power was set at an intermediate value of 80 W. In comparison, Sailor [62] reported metabolic heat power equal to 75 W at rest and 100–200 W in extreme activity alike Allen et al. [63] while Kikegawa et al. [34] set the metabolic heat rate equal to 54.7 W in their study. The maximum waste heat produced by building equipment is set at 36 W/m^2 for the all urban types as suggested by Salamanca et al. [60], who considered maximum wasted heat power equal to 36 W/m^2 and 20 W/m^2 for equipment in COI and HIR-LIR, respectively. In France, however, it seems that the amount of waste heat produced by building equipment per day is much lower, somewhere between 5.7 W/m^2 and 1.1 W/m^2 following CSTB [64]. Nonetheless, many uncertainties are attached to the specification of metabolic heat rate and the amount of waste heat produced by equipment. Finally, the daily profile of equipment usage was assumed to be constant for all the urban types in a day, although a daily "M" profile that varies according to the building function and homed socio-economic activities are also suggested by the French energy center, CSTB [64]. The parameterization of the BEM module does not permit a mix of residential and commercial activities inside buildings, as is often the case in cities.

Based on these settings, the WRF/urban climate modeling system computed the hourly air temperatures at height 2 m and the space heating energy demands of each urban grid cells of the Strasbourg Eurodistrict simulation domain.

3.2.2. Design of scenarios

The second step of our analysis was to design a set of scenarios reproducing typical energy conservation measures advocated in official building thermal regulations (*e.g.* improvement of the building insulation performance) as well as typical household behaviors regarding substitution energy (*e.g.* increase of the household thermal comfort expectations inside buildings induced by the impact of energy conservation measures on the relative energy price and household purchasing power).

The aim of this set of scenarios was twofold:

- To highlight the sensitivity of the city-scale degree-day model, in particular the base temperature, to the building thermal properties and thermostat settings in order to determine the optimal frequency of the city-scale degree-day model updates.
- To consider typical energy conservation measures advocated in official building thermal regulations, such as improvement of the insulation performance of the indoor and/or outdoor walls, as well as the effect of the relative energy price on the UHI and its impact on the space heating energy demands.

However, it should be noted that, in contrast to engineering building energy models, the BEM module is unable to account for real building designs, shading devices and operations. It considers a simplified cubic building geometry, a uniform positioning of windows on the four building faces regardless of the general orientation to the north or south for instance, and assumes a standard building occupancy pattern and thermal comfort expectation for all buildings of a particular urban type. Therefore, rather than realistic case studies, the designed scenarios represent ideal cases. Table 3 describes the scenarios.

4. Results and discussions

4.1. Analysis of the urban climate model results

Following Salamanca et al. [37], the 1 km^2 spatially averaged 2 m air temperature and wind speed simulations are directly compared with the punctual meteorological measurements provided by the national meteorological institute *Météo France*. Fig. 4. shows the locations of the three available monitoring stations in the Strasbourg Eurodistrict domain.

Table 4 provides the following statistics: the monthly Mean Biases (MBs) calculated as the mean differences between the hourly temperature simulations and observations for each month; the Root Mean Square Errors (RMSEs) of these differences; the Pearson coefficient of correlation (r) calculated on an annual basis. The Pearson coefficient of correlation r is equal to 0.96 for all stations for air temperature and 0.6 for the wind speeds. MBs are almost always below −1 °C. It is noted that disparities are greater for the station Strasbourg-Botanique located in the cool footprint of the Botanique garden as outlined by Fischer [65], thereby restricting its representativeness as a "dense urban" station within the WRF/urban climate model. MBs exhibit a seasonal pattern with slightly higher negative MBs during the vegetative period for Entzheim and La Wantzenau as compared to wintertime heating periods. According to the MBs and RMSEs, the wind speeds are bet-

Table 3
Description of the building design scenarios (HIR: high intensity residential city districts, LIR: low intensity residential city districts, and COI: commercial and industrial city estates).

Thermostat set point temperature	*Strasbourg base case* + Increase in the thermostat set point temperature by +1 °C (T1)	*Strasbourg base case* + Increase in the thermostat set point temperature by +2 °C (T2)
Wall insulation performance of the HIR and LIR buildings	Gypsum, a thin cavity layer of air, 32 cm bricks, and roughcast in cement U-value = 0.39 W m^{-2} K^{-1} (*No insulation*)	
	Gypsum, a thin cavity layer of air, 9 cm of glasswool insulation facing the indoor walls, 20 cm bricks, 3 cm cavity layer of air and roughcast in cement U-value = 0.19 W m^{-2} K^{-1} (*Interior insulation*)	Gypsum, a thin cavity layer of air, 20 cm bricks +9 cm of glasswool insulation facing the outdoor walls, 3 cm cavity layer of air and roughcast in cement U-value = 0.19 W m^{-2} K^{-1} (*Exterior insulation*)

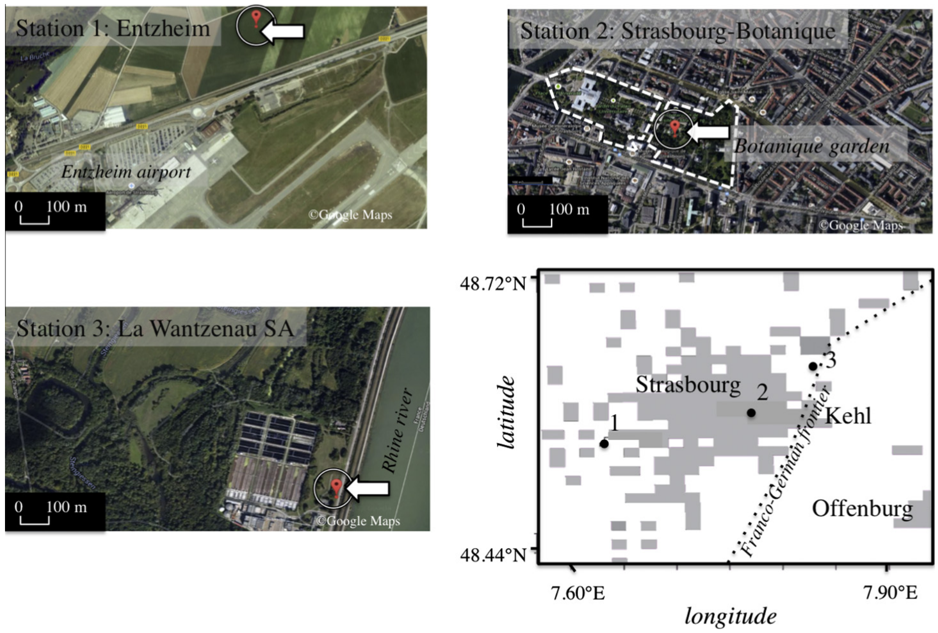

Fig. 4. Monitoring station sites and land cover characteristics. Station 1: Entzheim-airport (150 m, flat terrain, 48°33′N and 7°38′E). Station 2: Strasbourg-Botanique (139 m, green areas within the dense urban core of the main Strasbourg agglomeration, 48°35′N and 7°46′E). Station 3: La Wantzenau (135 m, north from the Robertsau Rhine hard flood forest which is 493 ha, 48°38′N and 7°50′E). The graphic represents the urban area of the Strasbourg Eurodistrict as seen by the WRF/urban climate modeling system. (For interpretation of the references to color in this figure legend, the reader is referred to the web version of this article.)

Table 4
Statistical comparisons of the observed and simulated hourly 2 m air temperatures and 10 m wind speeds for 2010: Mean biases (MBs) and Root Mean Square Errors (RMSEs).

	Air temperatures (in K)			Wind speeds (in m s^{-1})		
	Entzheim	*Strasbourg-Botanique*	*La Wantzenau*	*Entzheim*	*Strasbourg-Botanique*	*La Wantzenau*
MBs						
January	−0.45	2.03	0.31	0.27	–	1.36
February	−0.47	1.79	0.15	0.68	–	2.10
March	−1.17	0.76	−0.69	0.21	–	1.71
April	−1.61	0.81	−1.02	−0.58	–	0.68
May	−0.91	1.70	−0.19	−0.02	–	1.17
June	−1.25	1.90	−0.44	−0.46	–	0.93
July	−1.03	2.13	−0.18	−0.04	–	0.83
August	−0.91	2.20	0.32	0.10	–	1.36
September	−1.98	0.54	−0.77	0.01	–	1.01
October	−0.28	1.59	0.84	0.28	–	1.43
November	−0.22	2.16	0.47	0.75	–	1.95
December	−0.94	2.85	1.33	0.80	–	1.72
RMSEs						
January	1.78	2.78	1.86	1.86	–	4.46
February	1.86	2.60	1.95	4.08	–	8.07
March	2.42	2.31	2.30	3.80	–	5.33
April	2.73	2.40	2.45	3.09	–	3.07
May	2.14	2.61	1.85	2.43	–	4.62
June	2.29	2.82	1.89	2.60	–	4.32
July	2.64	3.29	2.44	1.96	–	2.70
August	2.28	2.99	2.00	2.41	–	4.33
September	2.	2.40	2.07	1.49	–	2.71
October	2.33	2.90	2.57	2.53	–	4.88
November	1.54	2.71	1.74	3.82	–	7.49
December	2.23	3.53	2.38	3.70	–	6.48

ter reproduced at Entzheim than at La Wantzenau. However, the wind speed sensor at Entzheim is more accurate than at La Wantzenau, explaining the high MBs and RMSEs at La Wantzenau.

The temperature and wind speed errors are comparable to those of other studies [37,66] and can be judged acceptable. Therefore, and despite the absence of a dense meteorological observation network over the domain, the WRF/urban climate modeling system is shown to reproduce accurate meteorological fields.

The simulations of demand for space heating energy gave an annual total for 2010 of 3,348,687 MWh. Compared to ASPA estimates, the simulations under-estimate the building space heating energy demands of the Strasbourg-Eurometropolis housing stock by up to −21.07%. The sensitivity analysis detailed in Section 4.3 will help to shed light on the differences.

4.2. The city-scale degree-day model and its validation

In order to construct the city-scale degree-day model, we plotted the city-scale daily building heating energy demands against the city-scale daily mean air temperatures as shown in Fig. 5.

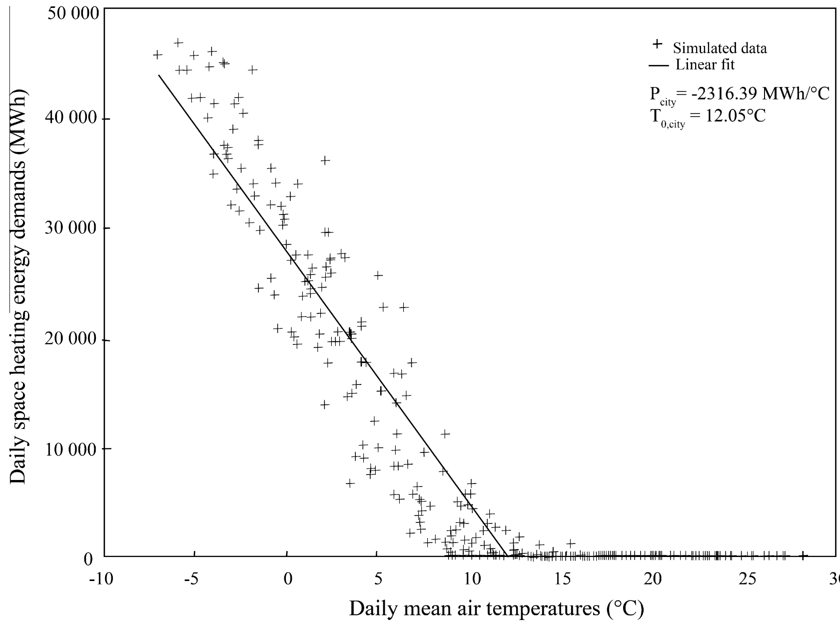

Fig. 5. The city-scale energy signature profile of the Strasbourg Eurometropolis area.

The correlation between decreasing building heating energy demands and rising air temperature follows a steep slope. At around 10 °C, the building heating energy demands rapidly become non-climate sensitive. For a given air temperature, the simulated building heating energy demands vary by ±10,000 MWh. This variation can be explained by the intermittent heating energy demands induced by the thermal inertia of the buildings and passive heat gains with respect to the varying weather conditions. Furthermore, below approx. 12 °C, a linear relationship can be assumed between the city-scale daily building heating energy demands and mean air temperatures.

Additionally, we linearly regressed the energy signature profile by considering only those days in the simulation dataset for which the city-scale daily building heating energy demands are not zero, meaning that the regression was made for 230 observations instead of the 365 observations as in the original dataset. From this linear model, we deduced the city-scale building heat loss rate P_{city}^{annual} and base temperature $T_{0,city}^{annual}$ for space heating suitable for the Strasbourg Eurometropolis housing stock. The city-scale building heat loss rate is then −2316.39 MWh/°C, and the city-scale base temperature is 12.05 °C. The Pearson coefficient of correlation was $r = 0.93$ (for a *p-value* $\ll 0.05$). These results are consistent with over official sources. A recent technical note of the French power delivery company RTE [67] indicates an average building heat loss rate equal to −2300 MWh/°C for the French housing stock, whilst in a Swiss study Christenson et al. [28] selected predefined base temperatures of 8 °C, 10 °C, and 12 °C.

To assess the quality of the city-scale degree-day model, we undertook a deeper analysis of the residuals. For this, we calculated the hat matrix (h_{ii}), which indicates the influence of each response value on the fitted value of the city-scale degree-day model. This shows the leverage effect of the coolest days for which the highest city-scale daily building space heating energy demands are observed (for $h_{ii} > 0.17$). This means that the accuracy of the city-scale degree-day model is largely dependent on the capacity of the WRF/urban climate modeling system to simulate the daily mean temperature of the coldest days and afferent space heating energy demands.

On the quantile-quantile diagram (Fig. 6) we observe a structural break in the residual distribution characterized by a major deviation (right-skewed distribution) from a normal distribution for the first and last quantiles (around −5 °C and 8 °C) due to the non-linearity of the space heating energy demand-air temperature relationship. This indicates an underestimate of the city-scale daily building space heating energy demands below −5 °C and above 8 °C when calculating the city-scale daily building space heating energy demands using the city-scale degree-day model. However, as stressed by CIBSE [31], while the discrepancies between the simulation and the city-scale degree-day model are more numerous near the base temperature, they are also smaller since the buildings are close to reach a thermal equilibrium with their surrounding ambient air conditions. This implies that the city-scale degree-day model perform well above −5 °C. If future daily means air temperatures become colder or fall more frequently below −5 °C, this will necessitate the development of an alternative city-scale degree-day model.

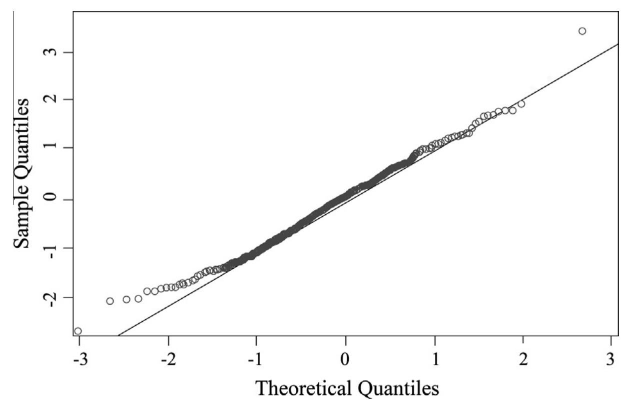

Fig. 6. Normal quantile-quantile diagram.

Although the discrepancies can be large for particular days, we focused on annual estimates, for which the errors should be minimized through linear regression by means of the least square residuals method. For the year 2010, we calculated an annual space heating energy demands Q_{2010}^{annual} using the city-scale degree-day model of 3,521,052 MW h. The discrepancy between the simulated heating energy demand EC_{2010} (*i.e.* 3,348,715 MW h) and the calculated space heating energy demands Q_{2010}^{annual} is +5.14%. In comparison, Valor et al. [25] reported discrepancies in the predicted building energy consumptions using their degree-day model of up to ±4%. Hence, our city-scale degree-day model provides accurate annually-based results compared to our simulations.

The ASPA also provided the total heating degree-days (HDD_{ASPA}) for 2010 used in their study. It is −1701.31 °C.days. In comparison, our figure of HDD_{WRF} = −1445.64 °C.days was up to -15.02% lower. Since the ASPA estimates can be written in similar way to Eq. (1), as:

$$Q_{2010}^{ASPA} \approx \sum_{t=0}^{t=nj}\sum_{nb=1}^{nb} P_b * min(T(t) - T_{0,b}) \tag{3}$$

where P_b and $T_{0,b}$ are the building heat loss rate and base temperature for each building type of the Strasbourg Eurometropolis housing stock, *nb*: the number of buildings, and *nj*: the number of days in a year, we recomputed a city-scale building heat loss rate P_{ASPA} at −2493.94 MWh/°C. The city-scale building heat loss rate calculated from data issued by ASPA (P_{ASPA}) is then slightly higher than the city-scale building heat loss rate calculated in our study (P_{WRF}) with relative differences between our study and ASPA of −7.11%. Therefore, more than the city-scale building heat loss rate, the HDD explains the differences in the building space heating energy demands between the two studies. These differences can either be attributed to the period of heating, the base temperature, or the definition of the daily mean temperature, and confirms the need for precise modeling of the UHI effect.

In order to deepen the analysis of the differences in the HDD, we performed a Stein and Alpert decomposition method [68]. The basic idea is to estimate the relative importance of each term of the HDD equations in regards to the total difference observed between the two studies. The global known difference, ΔHDD, between HDD_{WRF} and HDD_{ASPA} is assumed to be the sum of the influences of several parameters: $\Delta HDD^{\Delta t}$ = the difference in the HDD due to the predefined heating period, $\Delta HDD^{T(t)}$ = the difference due to the calculation of the daily mean air temperature as an average over 24 h of the hourly air temperatures or from the diurnal thermal amplitude (T_{minmax} method); ΔHDD^{T_0} = the difference due to the base temperature (12.05 °C instead of 17 °C as in ASPA); ΔHDD^{int} the difference due to non-linearity in the cumulative effects.

In this way, ΔHDD could be defined as:

$$\Delta HDD = \Delta HDD^{\Delta t} + \Delta HDD^{T(t)} + \Delta HDD^{T0} + \Delta HDD^{int} \tag{4}$$

Each term on the right of Eq. (4) was estimated using scenarios to simulate the hourly temperature simulations using the WRF/urban climate modeling system. First, a simulation was performed using the same methodology as ASPA and compared to a simulation as we proposed in this study. The difference gives an estimation of ΔHDD, called ΔHDD^*. Then several simulations were performed, in which each parameter was separately varied: heating period, use of daily maximum amplitude of temperature instead of mean temperature, base temperature. All of these simulations lead to varying estimates of HDD, that are respectively estimations $\Delta HDD^{\Delta t*}$, $\Delta HDD^{T(t)*}$, ΔHDD^{T0*}. An estimate of ΔHDD^{int*} could be easily calculating using Eq. (4). Considering all these estimates, we weighted them as compared to the real relative difference observed between the two methodologies. It turns out that the difference in the heating period is responsible for 0.1% of the 15,7% difference in HDD; the ASPA predefined base temperature explains −9.3%; and the definition of the daily mean air temperature explains −13.3%; the interaction term is non-negligible at 7% but also not explained. Thereby, the T_{minmax} method attributes much of the difference between the two studies (*i.e.* coarse assumption of quasi-sinusoidal diurnal temperature profile, [31] following by the predefined base temperature.

The much lower base temperature in our study compared to ASPA can be explained by the computation of the space heating energy demands through a three-dimensional UCP in which the mutual longwave radiative interactions between the buildings (UHI effects), as well as the other passive energy gains better predict the thermal inertia of the buildings and their intermittent demands for space heating energy. As other scholars already reported, the base temperature may vary according to the building thermal properties, the passive heat gains induced by solar radiations, people and equipment as well as the thermal comfort expectation inside the buildings [25,27,31].

4.3. Sensitivity and scenarios analysis

Additionally, we performed several sensitivity tests (described in Section 3.2.2) and computed both parameters of the city-scale degree-day model and estimates of the energy demand for space heating of the Strasbourg Eurometropolis' housing stock to get confidence in our city-scale degree-day model. Since a sensitivity study with several scenarios and demanding hourly simulations over a whole year requires massive computational resources, we shorten the time period on which the methodology is based (*i.e.* three months). For this, we iteratively calculated the city-scale building heat loss rate and base temperature for each combination of three months in a year. We chose a combination that minimizes the discrepancies with the city-scale building heat loss rate and base temperature calculated from the annual hourly simulations and the three months simulations. The selected months are February, March and September. The city-scale building heat loss rate $P_{city}^{3months}$ and base temperature $T_{0,city}^{3months}$ are then −2316.7 MWh/°C (relative difference compared to annual value: +0.01%) and 12.14 °C (relative difference compared to annual value: +0.74%), respectively. Using these values, and the urban-scale daily mean air temperatures over the year, we observed a slight overestimate of the annual city-scale space heating energy demands of the Strasbourg Eurometropolis housing stock (+1.17% for a space heating energy demand equal to $Q_{2010}^{3months}$ 3,562,299 MW h). The simulation solely for the three selected months gives accurate annual 2010 city-scale space heating energy demands.

Table 5 shows the impact of several scenarios on the city-scale degree-day model parameters, space heating energy demands, and city-scale daily mean air temperatures. If variations of energy demands in buildings for space heating and city-scale building heat loss rates confirmed well-known behavior already reported in previous works conducted at individual building scale (*e.g.* decreasing space heating energy demands in well-insulated buildings independently of the position of the insulating material in walls, increasing space heating energy demands with higher thermal comfort expectations inside buildings and windows apertures; [25,27,31,69–71], one can note that city-scale base temperatures $T_{0,city}$ and outdoor temperatures are varying too. The city-scale base temperature varies most when the thermal performance of buildings is improved (at maximum −30.30%) but also (in a non-negligible way) with increases in the thermal comfort expectations (at maximum +11.28%). Scenario T2, when the thermostat heating set point temperature is increased by +2 °C, shows the highest changes in the city-scale daily mean air temperatures. The minimum temperature shows an increase of +1 °C. The maximum temperature increases by +0.25 °C, and the first and third quartiles by +0.24 °C and +0.53 °C, respectively indicating a warming of the daily mean air temperature. The highest the thermostat tempera-

Table 5
City-scale space heating energy demands and parameters of the city scale degree-day model for the sensitivity scenarios. Additionally, the description of the statistical distribution of the city-scale daily mean air temperature is provided. Following, the total space heating energy demand simulated over the three months is $EC_{3months}$, the city-scale heat loss rates and base temperatures are $P_{city}^{3months}$ and $T_{0,city}^{3months}$, respectively. The estimate of energy demands in building for space heating over three months using the optimized 3-months city-scale degree-day model is $Q_{3months}$ and over the year 2010 $Q_{2010}^{3months}$. Errors induced by the use of the city-scale degree-day model are indicated in "*italic%*" while differences between scenarios in "regular%". Besides, T_{min} is the minimum temperature of the city-scale daily mean air temperatures, T_{max} its maximum, T_{mean} and T_{median} the mean and median air temperatures (respectively), while *q1* and *q3* are the first and third interquartiles.

	Scenarios					
	Reference case: No insulation	Interior insulation	Exterior insulation	Reference case: Strasbourg base case	T1	T2
Direct WRF-BEP-BEM results						
$EC_{3months}$ (MWh)	715,976	89,508 (−87.49%)	87,980 (−87.71%)	1,072,092	1,204,155 (+20.17%)	1,205,985 (+20.35%)
City scale degree-day results						
P_{city} (MWh °C^{-1})	−1886.7	−347.4 (−81.58%)	353.3 (−81.27%)	−2316.7	−2352.89 (+1.56%)	−2489.26 (+7.44%)
$T_{0,city}$ (°C)	10.56	7.66 (−27.46%)	7.36 (−30.30%)	12.14	13.01 (+7.16%)	13.51 (+11.28%)
$Q_{3months}$ (MWh)	738,503	91,097.9 (−87.68%)	88,856.3 (−87.96%)	1,106,969.6	1,254,287.5 (+13.30%)	1,257,976.1 (+13.64%)
$Q_{2010}^{3months}$ (MWh)	2,347,088	282,735.8 (−87.95%)	273,690.2 (−88.33%)	3,562,299.3	4,030,048.6 (+13.13%)	4,529,377.7 (+27.15%)
Comparisons between $EC_{3months}$ and $Q_{3months}$ (%)	+3.14%	+1.77%	+0,99%	+3.2%	+4.07%	+4.22%
City-scale daily mean air temperature (in °C)						
T_{min}	−5.84	−5.90	−5.89	−5.73	−5.72	−4.12
T_{max}	17.79	17.49	17.57	17.93	17.81	18.18
T_{mean}	7.42	7.38	7.39	7.45	7.55	7.88
T_{median}	9.00	9.04	9.09	9.15	9.08	9.30
q_1	1.89	1.79	1.88	1.91	1.92	2.15
q_3	12.49	12.47	12.66	12.59	12.90	13.12

ture is the warmest are the city-scale daily mean air temperatures: additional space heating demands in buildings, lead to more intense building heat losses in streets.

Furthermore, one can see that energy demands in buildings for space heating between T1 (when the thermostat heating set point temperature is increased by +1 °C) and T2 over the three simulated months $EC_{3months}$ are nearly the same: higher UHI effects in scenario T2 balances the higher space heating energy demands in buildings induced by the rise in the thermostat heating point temperature. Besides, $T_{0,city}$ although was found to be highly sensitive to the thermostat heating set point temperature in other studies solely increased by +0.5 °C for each +1 °C rise, suggesting high influence of UHI effects. While this finding is less clear when considered over the whole year, the daily mean air temperatures have also not been recomputed for the longer timeframe. Thus, variations of outdoor temperatures with the thermostat heating set point temperature, and the feedback impact on energy demand for space heating should be taken into account into energy conservation policies: lower thermostat heating temperatures can contribute towards low UHI and maybe enhanced energy demands in buildings for space heating in urban areas.

Last, improved building thermal insulation has the effect of slightly cooling the city-scale daily mean air temperatures (building heat losses are reduced in the building insulation scenarios and lower city-scale daily mean air temperatures are noted). Thus, although improved building insulation performance and massive walls reduce the sensitivity of space heating energy demands in buildings to outdoor air temperature variations, we aware that they also contribute to a global cooling of the city. It could be important to take into account this result when choosing heating system technologies. For instance, the performance of air source heat pumps often promoted in cities as low-carbon technology may be affected by outdoor temperature cooling [72,73].

4.4. Towards an application to fast compute impacts of climate variations on city-scale annual energy demands in buildings for space heating

Predictions of energy demands in buildings for space heating and at city-scale are suitable information to urban planners to frame optimized energy conservation policies: what are the current trend in energy demands for space heating in buildings in regards to climate variations? And what will be or could be future energy demands in buildings for space heating? In other words, on which annual space heating energy demand baselines should the energy conservation policies be framed?

To illustrate such application of the proposed method in urban planning and its performance to estimate energy demands in buildings for space heating in a quick fashion, we successively computed annual space heating energy demands of the Strasbourg Eurometropolis' housing stock over the 2011–2015 time period based on our city-scale degree-day model. We considered first the current meteorological conditions of the Strasbourg Eurometropolis, and second the meteorological conditions of Marseille (South of France) since it is expected that the climate of Marseille will be the one of Strasbourg Eurometropolis in 2100. In this application, we considered only changes in meteorological conditions and no changes in urban forms or in the energy performance of buildings. The meteorological conditions were taken from the synoptic meteorological stations: at Entzheim airport for the Strasbourg Eurometropolis, and at Marseille-Marignane airport (43°17′47″north and 5°22′12″east) for Marseille. These are directly available from the meteorological services' open source platform (https://donneespubliques.meteofrance.fr/) every 3 h, and are certainly more affordable for city planners than simulated city-scale daily mean air temperatures.

First, we adapt the parameters of our degree-day model to the use of air temperature observations instead of simulated data.

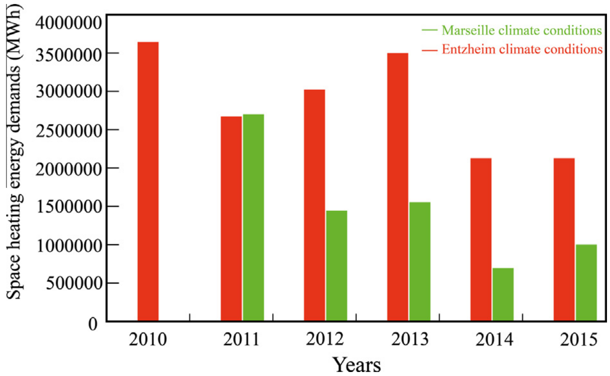

Fig. 7. Inter-annual variations of the energy demands for space heating of the Strasbourg Eurometropolis for the climate conditions of Entzheim and Marseille.

The new P_{city} (−2329.05 MWh/°C) and $T_{0,city}$ (11.61 °C) are then slightly higher and lower respectively than the P_{city} and $T_{0,city}$ of the base case since air temperatures at Entzheim are slightly cooler than the city-scale daily mean air temperatures. To account for this temperature difference in our city-scale annual energy demand estimates for space heating, two correction factors for the two parameters of the city-scale degree-day model were applied when computing the annual space heating energy demand of the Strasbourg Eurometropolis. There are 0.99 for P_{city} and 1.04 for $T_{0,city}$. Fig. 7 shows the resulting inter-annual variations of the space heating energy demands of the Strasbourg Eurometropolis considering the climate conditions of Entzheim and Marseille-Marignane airport. The graph shows that the annual energy demands for building space heating decrease slightly and in particular since 2013. Besides, if the Strasbourg Eurometropolis region will experience the same climate as Marseille, the annual energy demands for building space heating will be divided by approx. factor 2 solely due to the increase in temperatures. This can have a non-negligible impact on scales and financial subsides let at disposal for energy conservation measures. Furthermore, the suitability of our degree-day model in estimating in a quick fashion future energy demands in buildings for space heating is proven.

5. Conclusion

In this study, we develop a new degree-day method based on the WRF/urban climate modeling system and a Strasbourg Eurometropolis case study (France). This new method aims to estimate in a quick fashion the total energy demand in buildings for space heating of any city worldwide and time period considering in particular impacts of urban environments on the building outdoor temperatures (urban heat island effects, UHI) and space heating energy demands in buildings.

In our application and alike a classical degree-day method, hourly urban air temperatures and building energy demands for space heating were used to generate the energy signature profile of the Strasbourg Eurometropolis housing stock. We deduced from the latter, the average building heat loss rate (*i.e.* the city-scale building heat loss rate P_{city}) and base temperature (*i.e.* the city-scale base temperature $T_{0,city}$) suitable for the estimation of the space heating energy demand of the Strasbourg Eurometropolis' housing stock.

As a novelty of our method, hourly urban air temperatures and building energy demands for space heating are directly outputted from a regional urban meteorological model, the WRF/urban climate modeling system that accounts for the complex energy interactions between buildings and the urban atmosphere, *i.e.* the urban heat island (UHI). To work, the WRF/urban climate modeling system requires only few assumptions on the housing stock properties and building input data as compared to engineering building energy models. Based on our case study and sensitivity tests of our new degree-day method, several conclusions can be drawn.

Our method was first proven to give accurate estimates of annual building energy demand for space heating in the Strasbourg Eurometropolis' housing stock in 2010 as compared to other local official source and this, despite a moderate level description of the housing stock of the studied area. This is particularly interesting since this suggest that our method can also be suitable to predict space heating energy demands in buildings in part of the world where detailed housing stock description, long-term historical data of building energy demands for space heating/cooling and meteorological data are difficult to obtain and/or scarce. However and because the city-scale building heat loss rate P_{city} and base temperature $T_{0,city}$ (and in particular P_{city}) were showed to be mainly sensitive to the building insulating performance and thermal comfort expectations inside buildings, it is more than likely that the city-scale degree day model of the Strasbourg Eurometropolis will need regular update in future through along implementations of more stringent building thermal regulations and long terms acclimatization of individuals to ongoing climate change.

Considerations of UHI effects, although weaker in wintertime, on urban air temperatures and energy demands in buildings for space heating were found to be vital to accurately estimate the base temperature $T_{0,city}$ of the city-scale degree-day model and heating degree days. We calculated that non-considerations of UHI effects and resulting intermittent use of space heating energy in buildings contribute toward substantial overestimates of the base temperature (difference of 4 °C as compared to a local official source), and hence heating degree-days (+9.3%).

Building insulation performance significantly influences UHI effects and energy demands in buildings for space heating. Poor energy performing buildings contribute towards higher wasted heat in the atmosphere and higher UHI intensity than well-insulated buildings. While the cooling of the urban atmosphere has no impacts on space heating energy demands in well-insulated buildings, the warming of the urban atmosphere through building wasted heat can significantly reduce the space heating energy demands in poor energy performing buildings, at least in our configuration (the COP of the heating system is assumed constant, regardless of the temperature variations). Further investigations are required to assess the influence of the building insulation performance on the COP of the heating system and resulting space heating energy demands in buildings. However, it is more than likely that improved building insulation standards and building renovation programs may substantially modify the performance of the air-source heat pumps in cities by reducing the contribution of the wasted heat in the UHI phenomenon.

Finally, above a proposed illustrative study on the impact of climate change in the space heating energy demands in Strasbourg, we claim the proposed methodology can be used to help urban planners to frame optimized energy conservation strategies or furthermore, like in the country scale European Odyssee project [74] rank cities in regards to their space heating energy performance. This latter city benchmarking has already proven to promote energy efficiency through virtuous city competitions and attributions of green labeling. It is furthermore argued here that this city benchmarking can help to determine if the configuration of a city is more or less well adapted to temperature changes compare to another.

As further helpful applications of our method in urban planning, we think that our method can be spatialized (spatialized building heat loss rate P and base temperature T_0) to provide estimates of building energy demands for space heating at city-district scales and assess outcomes of small-scale urban renewal and building renovation policies implemented at parcel lots. For this, improved representations of the sub grid scale urban surface inhomogeneity in urban meteorological models are needed as well as validations of the methodology at the city district scale. Although the proposed method requires meteorological modeling and computational skills, we guess that the P and T_0 of the city districts of the main agglomerations of a country can be computed by its national meteorological institute and disclosed in an open source platform directly accessible to urban planners. More validation data are needed to demonstrate it.

Acknowledgments

Special thanks go to Alberto Martilli (CIEMAT, Madrid) for his expert advices on urban climate modeling, to Pascaline Clair (ASPA, Strasbourg) for her useful input for the study, Cécile Tannier (Chrono-environnement, Besançon) for her friendly recommendations, as well as to some anonymous reviewers. This work was supported by the French National Center for Scientific Research (CNRS), the French National Research Agency (ANR TVU), the European Union (FEDER ODIT-CEUP), the ZAEU Alsatian regional interdisciplinary research and inter-agency network, and the REALISE Alsatian regional network for environmental research. The authors are grateful to the regional air quality association ASPA, the meteorological institute Météo France, and the Strasbourg Eurometropolis, which provided free-of-charge large collections of high-resolution regional datasets. Simulations were performed at the high-performance computing facilities of the Université de Strasbourg.

References

[1] Taylor JW, De Menezes LM, McSharry PE. A comparison of univariate methods for forecasting electricity demand up to a day ahead. Int J Forecast 2006;22:1–16. doi: http://dx.doi.org/10.1016/j.ijforecast.2005.06.006.
[2] European commission. Directive 2010/31/UE sur la performance énergétique des bâtiments. Journal officiel de l'Union Européenne 2010;L153(13):23.
[3] European commission. Directive 2012/27/UE relative à l'efficacité énergétique. Journal officiel de l'Union Européenne 2012;L315(1):56.
[4] Pérez-Lombard L, Ortiz J, Pout C. A review on building energy consumption information. Energy Build 2008;40:394–8. doi: http://dx.doi.org/10.1016/j.enbuild.2007.03.007.
[5] Herrando M, Canbra d, Navarro M, de la Cruz L, Millan G, Zabalza I. Energy performance certification of faculty buildings in Spain: the gap between estimated and real energy consumption. Energy Convers Manage 2016. doi: http://dx.doi.org/10.1016/j.enconman.2016.04.037 [in press].
[6] Shahmohamadi P, Che-Ani AI, Ramly A, Maulud KNA, Mohd-Nor MFI. Reducing urban heat island effects: a systematic review to achieve energy consumption balance. Int J Phys Sci 2010;5(6):626–36.
[7] Oke TR. The energetic basis of the urban heat island. Quart J R Meteor Soc 1982;108(455):1–24. doi: http://dx.doi.org/10.1002/qj.49710845502.
[8] Ewing R, Rong F. The impact of urban form on US residential energy use. Housing Policy Debate 2008;19(1):45–52. doi: http://dx.doi.org/10.1080/10511482.2008.951626.
[9] Santamouris M, Papnikolaou N, Livada I, Koronakis I, Georgakis C, Argiriou A, et al. On the impact of urban climate on the energy consumption of buildings. Sol Energy 2001;70(3):201–16.
[10] Kolotroni M, Ren X, Davies M, Mavrogianni A. London's urban heat island: impact on current and future energy consumption in office buildings. Energy Build 2012;47:302–11. doi: http://dx.doi.org/10.1016/j.enbuild.2011.12.019.
[11] Ihara T, Kikegawa Y, Asahi K, Genchi Y, Kondo H. Changes in year-round air temperature and annual energy consumption in office building areas by urban heat island countermeasures and energy saving measures. Appl Energy 2008;85:12–25. doi: http://dx.doi.org/10.1016/j.apenergy.2007.06.012.
[12] Magli S, Lodi C, Lombroso L, Muscio A, Teggi S. Analysis of the urban heat island effects on building energy consumption. Int J Energy Environ Eng 2015;6:91–9. doi: http://dx.doi.org/10.1007/s40095-014-0154-9.
[13] Goy S, Finn D. Estimating demand response potential in building clusters. Energy Proc 2015;78:3391–6. doi: http://dx.doi.org/10.1016/j.egypro.2015.11.756.
[14] Swan LG, Ugursal VI. Modeling of end-use energy consumption in the residential sector: a review of modeling techniques. Renew Sustain Energy Rev 2009;13:1819–35. doi: http://dx.doi.org/10.1016/j.rser.2008.09.033.
[15] Kavgic M, Mavrogianni A, Mumovic D, Summerfield A, Stevanovic Z, Djurovic-Petrovic M. A review of bottom-up building stock models for energy consumption in the residential sector. Build Environ 2010;45:1683–97. doi: http://dx.doi.org/10.1016/j.buildenv.2010.01.021.
[16] Wang S, Chengchu Y, Xiao F. Quantitative energy performance assessment methods for existing buildings. Energy Build 2012;55:873–88.
[17] Kazas G, Fabrizio E, Perino M. Energy demand profiles assessment at district scale: a stochastic approach for a block of buildings demand profiles generation. Energy Proc 2015;78:3410–5. doi: http://dx.doi.org/10.1016/j.egypro.2015.11.610.
[18] Moreci E, Ciulla G, Lo Brano V. Annual heating energy requirements of office buildings in a European climate. Sustain Cities Soc 2016;20:81–95. doi: http://dx.doi.org/10.1016/j.scs.2015.10.005.
[19] Shimoda Y, Fujii T, Morikawa T, Mizuno M. Residential end-us energy simulation at city scale. Build Environ 2004;39:959–67. doi: http://dx.doi.org/10.1016/j.buildenv.2004.01.020.
[20] Mastrucci A, Baume O, Stazi F, Leopold U. Estimating energy savings for the residential building stock of an entire city: a GIS-based statistical downscaling approach applied to Rotterdam. Energy Build 2014;75:358–67.
[21] Mata E, Sasic Kalagasidis A, Johnsson F. Building-stock aggregation through archetype buildings: France, Germany, Spain, and the UK. Build Environ 2014;81(270):282.
[22] Han Y, Taylor JE, Pisello AL. Exploring mutual shading and mutual reflection inter-building effects on building energy performance. Appl Energy 2015. doi: http://dx.doi.org/10.1016/j.apenergy.2015.10.170 [in press].
[23] Pisello AL, Taylor JE, Xu X, Cotana F. Inter-building effect: simulating the impact of a network of buildings on the accuracy of building energy predictions. Build Environ 2012;58:37–45. doi: http://dx.doi.org/10.1016/j.buildenv.2012.06.017.
[24] Van der Heijden MGM, Blocken B, Hensen JLM. Towards the integration of the urban heat island in building energy simulations. In: Proceedings of BS2013: 13th conference of international building performance simulation association, August 26–28, Chambéry, France.
[25] Valor E, Meneu V, Caselles V. Daily air temperature and electricity load in Spain. J Appl Meteorol 2001;40(8):1413–21. doi: http://dx.doi.org/10.1175/1520-0450(2001) 040<1413:DATAEL>2.0.CO;2.
[26] Cartalis C, Synodinou A, Proedrou M, Tsangrassoulis A, Santamouris M. Modifications in energy demand in urban areas as a result of climate changes: an assessment for the southeast Mediterranean region. Energy Convers Manage 2001;42(14):1647–56. doi:10.1016:S0196-8904(00)00156-4.
[27] Amato AD, Ruth M, Kirshen P, Horwitz J. Regional energy demand responses to climate change: methodology and application to the commonwealth of Massachusetts. Clim Change 2005;71(1):175–201. doi: http://dx.doi.org/10.1007/s10584-005-5931-2.
[28] Christenson M, Manz H, Gyalistras D. Climate warming impact on degree-days and building energy demand in Switzerland. Energy Convers Manage 2006;47(6):671–86. doi: http://dx.doi.org/10.1016/j.enconman.2005.06.009.
[29] Quayle RG, Diaz HF. Heating degree day data applied to residential heating energy consumption. J Appl Meteorol 1980;19(3):241–6. doi: http://dx.doi.org/10.1175/1520-0450(1980) 019<0241:HDDDAT>2.0.CO;2.
[30] De Rosa M, Bianco V, Scarpa F, Tagliafico LA. Historical trends and current state of heating and cooling degree days in Italy. Energy Convers Manage 2015;90:323–35. doi: http://dx.doi.org/10.1016/j.enconman.2014.11.022.
[31] CIBSE. Degree-days: theory and application. Technical report TM41:2006, 2006. ISBN-10:1-903287-76-6..
[32] EUROSTAT. Energy statistics - heating degree-days, <http://ec.europa.eu/eurostat/cache/metadata/en/nrg_esdgr_esms.htm>; 2012 [last consultation: 28.07.2016].
[33] Giannakopoulos C, Hadjinicolaou P, Zerefos SC, Demosthenous G. Changing energy requirements in the Mediterranean under changing climatic conditions. Energies 2009;2:805–15. doi: http://dx.doi.org/10.3390/en20400805.
[34] Kikegawa Y, Genchi Y, Yoshikado H, Kondo H. Development of a numerical simulation system toward comprehensive assessments of urban warming countermeasures including their impacts upon the urban buildings' energy demands. Appl Energy 2003;76(4):449–66. doi: http://dx.doi.org/10.1016/S0306-2619(03)00009-6.
[35] Bueno B, Pigeon G, Norford LK, Zibouche K. Development and evaluation of a building energy model integrated in the TEB scheme. Geoscient Model Develop Disc 2011;4(4):2973–3011. doi: http://dx.doi.org/10.5194/gmdd-4-2973-2011.
[36] Salamanca F, Krpo A, Martilli A, Clappier A. A new building energy model coupled with an urban canopy parameterization for urban climate simulations: part I. Formulation, verification, and sensitivity analysis of the model. Theoret Appl Climatol 2010;99(3–4):331–44. doi: http://dx.doi.org/10.1007/s00704-009-0142-9.
[37] Salamanca F, Martilli A, Tewari M, Chen F. A study of the urban boundary layer using different urban parameterizations and high-resolution urban canopy parameters with WRF. J Appl Meteorol Climatol 2011;50(5):1107–28. doi: http://dx.doi.org/10.1175/2010JAMC2538.1.
[38] Masson V, Marchadier C, Adolphe L, Aguejdad R, Avner P, Bonhomme M, et al. Adapting cities to climate change: a systematic modeling approach. Urban Climate 2014;10(2):407–29. doi: http://dx.doi.org/10.1016/j.uclim.2014.03.004.
[39] Martilli A. An idealized study of city structure, urban climate, energy consumption, and air quality. Urban Climate 2014;10:430–46. doi: http://dx.doi.org/10.1016/j.uclim.2014.03.003.

[40] Yang B, Zhang Y, Qian Y. Simulation of urban climate with high-resolution WRF model: a case study in Nanjing, China. Asia-Pacific J Atmos Sci 2012;48 (3):227–41. doi: http://dx.doi.org/10.1007/s13143-012-0023-5.
[41] Hamdi R, Deckmyn A, Termonia P, Demarée G, Baguis P. Effects of historical urbanization in the Brussels Capital region on surface air temperature time series: a model study. J Appl Meteorol Climatol 2009;48:2181–96. doi: http://dx.doi.org/10.1175/2009JAMC2140.1.
[42] Lemonsu A, Kounkou-Arnaud R, Desplat J, Salagnac JL, Masson V. Evolution of the Parisian urban climate under a global changing climate. Clim Change 2013;116(3–4):679–92. doi: http://dx.doi.org/10.1007/s10584-012-0521-6.
[43] Ikeda R, Kuska H. Proposing the simplification of the multilayer urban canopy model: intercomparison study of four models. J Appl Meteorol Climatol 2010;49(5):902–19. doi: http://dx.doi.org/10.1175/2009JAMC2336.1.
[44] De Ridder K, Lauwaet D, Maiheu B. UrbClim–a fast urban boundary layer climate model. Urban Climate 2015;12:21–48. doi: http://dx.doi.org/10.1016/j.uclim.2015.01.001.
[45] Bueno B, Hidalgo J, Pigeon G, Norford L, Masson V. Calculation of air temperatures above the urban canopy layer from measurements at a rural operational weather station. J Appl Meteorol Climatol 2013;52(2):472–83. doi:10.1175:JAMC-D-12-083.1.
[46] Thom HCS. The rational relationship between heating degree-days and temperature. Mon Weather Rev 1954;82(1):1–6. doi: http://dx.doi.org/10.1175/1520-0493(1954) 082<0001:TRRBHD>2.0.CO;2.
[47] Day AR, Knight I, Dunn G, Gaddas R. Improved methods for evaluating base temperature for use in building energy performance lines. Build Serv Eng Res Technol 2003;24:221–8. doi: http://dx.doi.org/10.1191/0143624403bt073oa.
[48] Lee K, Baek HJ, Cho C. The estimation of base temperature for heating and cooling degree-days for South Korea. J Appl Meteorol Climatol 2014;53:300–9. doi: http://dx.doi.org/10.1175/JAMC-D-13-0220.1.
[49] Azevedo JA, Chapman L, Muller CL. Critique and suggested modifications of the degree-days methodology to enable long-term electricity consumption assessments: a case study in Birmingham, UK. Meteorol Appl 2015;22 (4):789–96. doi:10.1002:met.1525.
[50] Skamarock WC, Klemp JB, Dudhia J, Gill DO, Barker DM, Duda M, et al. A description of the advanced research wrf version 3. Technical report, NCAR Technical Note. NCAR/TN-475+STR; 2008. doi:10.5065:D68S4MVH.
[51] Martilli A, Clappier A, Rotach MW. An urban surface exchange parameterisation for mesoscale models. Bound-Layer Meteorol 2002;104 (2):261–304. doi: http://dx.doi.org/10.1023/A:1016099921195.
[52] ASPA. Méthodologie de calcul des consommations d'énergie dans le secteur résidentiel- version v2012. Technical report, 2012 also available for some parts in <http://www.atmo-alsace.net/medias/produits/Consommations_denergie_.pdf, last consultation>; 2012 [19/07/2016].
[53] Grell GA, Dudhia J, Stauffer DR, et al. A description of the fifth-generation Penn state/NCAR mesoscale model (MM5), technical note NCAR/TN-398+STR, 1994.
[54] Dudhia J. Numerical study of convection observed during the winter monsoon experiment using a mesoscale two dimensional model. J Atmos Sci 1989;46:3077–107. doi: http://dx.doi.org/10.1175/1520-0469(1989) 046<3077:NSOCOD>2.0.CO;2.
[55] Thompson G, Rasmussen RM, Manning K. Explicit forecasts of winter precipitation using an improved bulk microphysics scheme. Part I: description and sensitivity analysis. Mont Weat Rev 2004;132(2):519–42. doi: http://dx.doi.org/10.1175/1520-0493(2004) 132<0519:EFOWPU>2.0.CO;2.
[56] Bougeault P, Lacarrère P. Parameterization of orography-induced turbulence in a mesobeta–scale model. Mon Weather Rev 1989;117(8):1872–90. doi: http://dx.doi.org/10.1175/1520-0493(1989) 117<1872:POOITI>2.0.CO;2.
[57] Chen F, Dudhia J. Coupling an advanced land surface-hydrology model with the Penn-NCAR MM5 modeling system. Part I: model implementation and sensitivity. Mont Weat Rev 2001;129:569–85. doi: http://dx.doi.org/10.1175/1520-0493(2001) 129<0569:CAALSH>2.0.CO;2.
[58] Suisse Energie. Catalogue valeurs U: détermination simple de la valeur U d'éléments de construction Technical Report, 2016 [24 p.].
[59] Dujin A, Maresca B. La température du logement ne dépend pas de la sensibilité écologique. Technical report –CREDOC: Consommation et mode de vie, 4 p., 2010.ISSN 0295–9976; 2010.
[60] Salamanca F, Martilli A, Yagüe C. A numerical study of the urban heat island over Madrid during the DESIREX (2008) campaign with WRF and an evaluation of simple mitigation strategies. Int J Climatol 2012;32(15):2372–86. doi: http://dx.doi.org/10.1002/joc.3398.
[61] INSEE. Aire urbaine de Strasbourg: une population qui augmente. Technical Report Chiffres pour l'Alsace, revue N°42: 7-10, 2007; 2007.
[62] Sailor DJ. A review of methods for estimating anthropogenic heat and moisture emissions in the urban environment. Int J Climatol 2011;31(2):189–99. doi: http://dx.doi.org/10.1002/joc.2106.
[63] Allen L, Lindberg F, Grimmond CSB. Global to city scale urban anthropogenic heat flux: model and variability. Int J Climatol 2011;31(13):1990–2005. doi: 10.1002:joc.2210.
[64] CSTB. Méthode de calcul th-bce 2012 Technical report, 2012. p. 1377.
[65] Fischer L. Etude de paramètres climatiques pertinents en vue de l'amélioration de la prévision des pointes de pollution par l'ozone dans l'agglomération de Strasbourg Thèse de doctorat. de l'Université Louis Paster.; 2001.
[66] Lemonsu A, Viguié V, Daniel M, Masson V. Vulnerability to heat waves: impact of urban expansion scenarios on urban heat island and heat stress in Paris (France). Urban Climate 2015;14:586–605. doi: http://dx.doi.org/10.1016/j.uclim.2015.10.007.
[67] RTE. Bilan électrique 2012 Technical report, 2012 [p. 44.].
[68] Stein U, Alpert P. Factor separation in numerical simulations. J Atmos Sci 1993;50(14):2107–15. doi: http://dx.doi.org/10.1175/1520-0469 (1993) 050<2107:FSINS>2.0.CO;2.
[69] Bojic M, Yik F, Sat P. Influence of thermal insulation position in building envelope on the space cooling of high-rise residential buildings in Hong Kong. Energy Build 2001;33(6):569–81. doi: http://dx.doi.org/10.1016/S0378-7788(00)00125-0.
[70] Sailor DJ, Pavlova AA. Air conditioning market saturation and long-term response of residential cooling energy demand to climate change. Energy 2003;28(9):941–51. doi:10.1016:S0360-5442(03)00033-1.
[71] Aste N, Angelotti A, Buzzetti M. The influence of the external walls thermal inertia on the energy performance of well insulated buildings. Energy Build 2009;41(11):1181–7. doi: http://dx.doi.org/10.1016/j.enbuild.2009.06.005.
[72] Bertsch SS, Groll EA. Two-stage air-source heat pump for residential heating and cooling applications in northern U.S. climates. Int J Refrig 2008;31:1282–92. doi: http://dx.doi.org/10.1016/j.ijrefrig.2008.01.006.
[73] Jenkins D, Tucker R, Ahadzi M, Rawlings R. The performance of air-source heat pumps in current and future offices. Energy Build 2008;40:1901–10. doi: http://dx.doi.org/10.1016/j.enbuild.2008.04.015.
[74] Enerdata. Odyssee database on energy efficiency data and indicators, <http://www.indicators.odyssee-mure.eu/benchmarking.html>; 2016.
[75] Krpo A. Development and application of a numerical simulation system to evaluate the impact of anthropogenic heat fluxes on urban boundary layer climate Ph.D. thesis. Ecole Polytechnique Fédérale de Lausanne; 2009 [233 pages].

Glossary

Acronyms
ASPA: Association pour la Surveillance et l'étude de la pollution atmosphérique en Alsace
BEM: Building Energy Model
BEP: Building Effect Parameterization
CEREN: Centre d'Etude et de Recherches économiques sur l'ENergie
CIBSE: Chartered Institution of Building Services Engineers
CIGAL: Coopérations pour l'Information Géographique en ALsace
COI: COmmercial and Industrial city estates
CSTB: Centre Scientifique et Technique du Bâtiment
HDD: Heating degree-days
HIR: High intensity residential city districts
INSEE: Institut National de la Statistique et des Etudes Economiques
IGN: Institut National de l'information Géographique et forestière
LIR: Low intensity residential city districts
MBs: Mean bias
MM5: The PSU/NCAR Mesoscale Meteorological model
NCEP: The National Centers for Environmental Prediction
Noah-LSM: The Noah Land Surface Model
RMSE: Root mean square errors
RTE: Réseau de Transport d'Electricité
SPOT: Système Probatoire d'Observation de la Terre
UCP: Urban canopy parameterization
UHI: Urban Heat Island
WRF/ARW: Advanced Weather Research and Forecasting model

List of variables
EC_{2010}: Total 2010 space heating energy demand calculated from the arithmetic sum of hourly space heating energy simulations
HDD_J: Heating degree-days over a period J
HDD_{ASPA}: Heating degree-days taken into account in the ASPA study
HDD_{WRF}: Heating degree-days calculated in our study
hii: Hat matrix for the analysis of the residuals of the linear fit
P: Spatialized building heat loss rate at district scale
P_b: Building-scale building heat loss rate
P_{city}: City-scale building heat loss rate
P_{ASPA}: City-scale building heat loss rate considered by the ASPA study
P_{WRF}: City-scale building heat loss rate considered in our study
P_{city}^{annual}: City-scale building heat loss rate calculated from the annual energy and air temperature simulations.
$P_{city}^{3months}$: City-scale building heat loss rate calculated from the energy and air temperature simulations of three selected months.
Q_J: Total space heating energy demand over a period J calculated form a degree-day method
Q_{2010}^{annual}: Total space heating energy demand for 2010 estimated from the city-scale degree-day model and the P_{city}^{annual} and $T_{0,city}^{annual}$.
$Q_{2010}^{3months}$: Total space heating energy demand for 2010 estimated from the city-scale degree-day model and the $P_{city}^{3months}$ and $T_{0,city}^{3months}$.
r: Pearson coefficient of correlation.
$T(t)$: Mean temperature of day t.
T_0: Spatialized base temperature at district scale
$T_{0,b}$: Building-scale base temperature

$T_{\mathbf{0,city}}$: City-scale base temperature
$T_{0,city}^{annual}$: City-scale base temperature calculated from the annual energy and air temperature simulations.
$T_{0,city}^{3months}$: City-scale base temperature calculated from the energy and air temperature simulations of three selected months.
U-value: Thermal transmissivity of a building wall
ΔHDD: Global differences between the $HDD_{\mathbf{ASPA}}$ and the $HDD_{\mathbf{WRF}}$
$\Delta HDD^{\Delta t}$: Differences in the $HDD_{\mathbf{ASPA}}$ and the $HDD_{\mathbf{WRF}}$ due to the period of heating Δt
$\Delta HDD^{T(t)}$: Differences in the $HDD_{\mathbf{ASPA}}$ and the $HDD_{\mathbf{WRF}}$ due to the daily mean temperature definition
ΔHDD^{T_0}.: Differences in the $HDD_{\mathbf{ASPA}}$ and the $HDD_{\mathbf{WRF}}$ due to the base temperature
ΔHDD^{int}: Differences in the $HDD_{\mathbf{ASPA}}$ and the $HDD_{\mathbf{WRF}}$ due to combined effect of all the parameters mentioned above.